Human Molecular Genetics, 2016, Vol. 25, No. 20 4546–4555

doi: 10.1093/hmg/ddw282
Advance Access Publication Date: 22 August 2016
Original Article

ORIGINAL ARTICLE

Mutations in the polyglutamylase gene *TTLL5*, expressed in photoreceptor cells and spermatozoa, are associated with cone-rod degeneration and reduced male fertility

Nicola Bedoni[1,†], Lonneke Haer-Wigman[2,3,†], Veronika Vaclavik[4,5], Viet H. Tran[4], Pietro Farinelli[1], Sara Balzano[1], Beryl Royer-Bertrand[1,6], Mohammed E. El-Asrag[7], Olivier Bonny[8], Christos Ikonomidis[9], Yan Litzistorf[9], Konstantinos Nikopoulos[1], Georgia G. Yioti[10], Maria I. Stefaniotou[10], Martin McKibbin[11], Adam P. Booth[12], Jamie M. Ellingford[13], Graeme C. Black[13], Carmel Toomes[7], Chris F. Inglehearn[7], Carel B. Hoyng[14], Nathalie Bax[14], Caroline C.W. Klaver[14,15], Alberta A. Thiadens[15], Fabien Murisier[16], Daniel F. Schorderet[17], Manir Ali[7], Frans P.M. Cremers[2,3], Sten Andréasson[18], Francis L. Munier[4,†] and Carlo Rivolta[1,†,*]

[1]Department of Computational Biology, Unit of Medical Genetics, University of Lausanne, Lausanne, Switzerland, [2]Department of Human Genetics, Radboud University Medical Center, Nijmegen, the Netherlands, [3]Donders Institute for Brain, Cognition and Behaviour, Radboud University, Nijmegen, the Netherlands, [4]Jules Gonin Eye Hospital, Lausanne, Switzerland, [5]Department of Ophthalmology, Fribourg Hospital HFR, Fribourg, Switzerland, [6]Center for Molecular Diseases, Department of Pediatrics, Lausanne University Hospital (CHUV), Lausanne, Switzerland, [7]Section of Ophthalmology & Neuroscience, Leeds Institute of Biomedical & Clinical Sciences, University of Leeds, Leeds, UK, [8]Service of Nephrology, Lausanne University Hospital (CHUV), Lausanne, Switzerland, [9]Department of Otorhinolaryngology, Head and Neck Surgery, Lausanne University Hospital (CHUV), Lausanne, Switzerland, [10]Department of Ophthalmology, University of Ioannina School of Medicine, Ioannina, Greece, [11]The Eye Department, St. James's University Hospital, Leeds, UK, [12]Royal Eye Infirmary, Derriford Hospital, Plymouth, UK, [13]Centre for Genomic Medicine, St. Mary's Hospital, Manchester Academic Health Science Centre, University of Manchester, Manchester, UK, [14]Department of Ophthalmology, Radboud University Medical Center, Nijmegen, the Netherlands, [15]Department of Ophthalmology, Erasmus Medical Center, Rotterdam, the Netherlands, [16]Fertas Andrology Laboratory, Lausanne, Switzerland, [17]Institute for Research in Ophtalmology, University of Lausanne and Ecole Polytechnique Federale de Lausanne, Switzerland and [18]Department of Ophthalmology, Lund University, Lund, Sweden

[†]The authors wish it to be known that, in their opinion, the first 2 authors and last 2 authors should be regarded as joint First and Last Authors, respectively.
Received: July 8, 2016. **Revised:** August 19, 2016. **Accepted:** August 20, 2016

*To whom correspondence should be addressed at: Carlo Rivolta, Department of Computational Biology, Unit of Medical Genetics, University of Lausanne, Rue du Bugnon 27, 1011 Lausanne, Switzerland. Tel: +41-21-6925451; Fax: +41-21-6925455; Email: carlo.rivolta@unil.ch

Abstract

Hereditary retinal degenerations encompass a group of genetic diseases characterized by extreme clinical variability. Following next-generation sequencing and autozygome-based screening of patients presenting with a peculiar, recessive form of cone-dominated retinopathy, we identified five homozygous variants [p.(Asp594fs), p.(Gln117*), p.(Met712fs), p.(Ile756Phe), and p.(Glu543Lys)] in the polyglutamylase-encoding gene *TTLL5*, in eight patients from six families. The two male patients carrying truncating *TTLL5* variants also displayed a substantial reduction in sperm motility and infertility, whereas those carrying missense changes were fertile. Defects in this polyglutamylase in humans have recently been associated with cone photoreceptor dystrophy, while mouse models carrying truncating mutations in the same gene also display reduced fertility in male animals. We examined the expression levels of *TTLL5* in various human tissues and determined that this gene has multiple viable isoforms, being highly expressed in testis and retina. In addition, antibodies against TTLL5 stained the basal body of photoreceptor cells in rat and the centrosome of the spermatozoon flagellum in humans, suggesting a common mechanism of action in these two cell types. Taken together, our data indicate that mutations in *TTLL5* delineate a novel, allele-specific syndrome causing defects in two as yet pathogenically unrelated functions, reproduction and vision.

Introduction

Cone dystrophies (CDs) and cone-rod dystrophies (CRDs) are rare heterogeneous retinal disorders with an estimated prevalence of ~1:40,000 (1). They lead to severe visual impairment, primarily or exclusively due to the degeneration of cone photoreceptors. Patients experience progressive loss of visual acuity, defective colour vision, photophobia, and have central scotomas. Only later, as the disease progresses, in some cases loss of peripheral vision may also occur (2,3).

The progressive degeneration of retinal photoreceptors in CDs and CRDs is mostly nonsyndromic and has been associated with multiple genetic causes, with at least 20 associated disease genes (RetNet; http://www.sph.uth.tmc.edu/RetNet/; date last accessed July 8, 2016). However, more than 75% of cases presenting with dominant or recessive forms of these conditions are genetically unsolved (4). Recent discoveries in CD molecular genetics include the identification of pathogenic variants in the tubulin polyglutamylase *TTLL5* (Tubulin Tyrosine Ligase-Like Protein 5) gene, found to cause retinal dystrophy in four British families (5). This gene, like the 12 other members of the TTLL superfamily, is involved in post-translational modifications of α- and β-tubulin, which are components of the axonemes of both cilia and flagella.

Interestingly, male mice with a defective TTLL5 display dramatically reduced fertility associated with defects in sperm motility (6). Most sperm tails of mutant mice were found to have disrupted axonemes with loss of tubulin doublets and a significantly decreased polyglutamylation in the upper and lower segments. No abnormal phenotype of retinal photoreceptors or of cochlear cells was initially observed, based on histologic examination (6). A second study with a more thorough characterization of the ocular phenotype in the same mouse model showed a decline of electroretinographic (ERG) amplitudes for both rods and cones in aged mice (20-22 mo). However, no microtubule defects were found after examination of electron micrographs (7).

Ciliopathies represent a class of hereditary disorders involving deficiencies in ciliary and cilia-associated proteins, often affecting a variety of tissues and organs (8). Due to the presence of an immotile cilium in both rods and cones photoreceptors, many ciliopathies display a retinal phenotype, either as part of a syndromic condition (associated with hearing defects, renal nephronophtisis, liver fibrosis, bone and/or brain anomalies) or as the sole pathological sign (9–11).

Following the investigation of a cohort of patients displaying CD or CRD, we identified mutations in *TTLL5* that are associated with both retinal degeneration and reduced sperm motility in humans, possibly defining a novel syndromic ciliopathy.

Results

Clinical and molecular findings

Our research started with the molecular characterization of a Swiss male patient (P1), aged 75 years, presenting with a late-onset cone dystrophy (CD). He was the eldest of three brothers and his parents were first cousins (Fig. 1, F1), without any history of ocular problems. The patient was first seen at the age of 33 years, when he first noticed blurred vision. His best corrected Snellen visual acuity (BCVA) at that time was 0.6 in the right eye and 0.8 in his left eye. Seven years later, his BCVA was still stable, but worsened when he was 53 years old, dropping dramatically to 0.05 in the right eye and 0.08 in the left eye. He was also complaining of a reduced dark adaptation. Twenty-two years later his vision remained stable, with the patient using more of his peripheral vision.

The clinical examination was typical of a cone dystrophy: the fundus examination showed central foveal atrophy with peripapillary hyperpigmentation and atrophy, while the peripheral retina was within normal limits (Fig. 2). The first ERGs (performed when the patient was 56 years old) showed normal scotopic responses, whereas photopic responses had severely reduced amplitude. The following ERG testing, when the patient was 70 years old, showed some rod involvement, with reduced rod-specific b-wave. The 30-Hz flicker was undetectable. Autofluorescent (AF) images at age 66 years (Fig. 2) showed central hypofluorescence corresponding to atrophy, surrounded by a large hyperfluorescent ring. AF imaging at age 72 indicated that the ring mildly increased in diameter, and so did the area of hypofluorescence (Fig. 2). Kinetic visual field tested at this later age showed mild constriction and central scotoma in both eyes.

The DNA of the patient was first screened for mutations in known disease genes. Following the negative output of a panel-

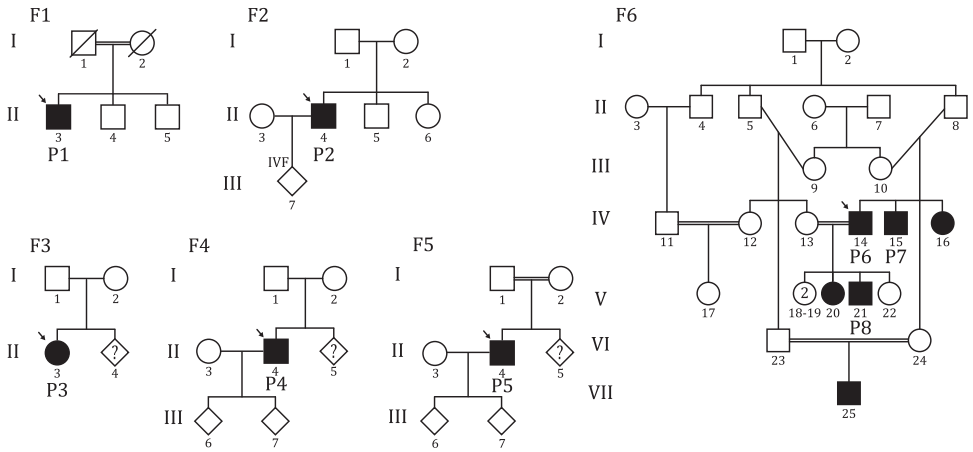

Figure 1. Pedigrees from families with pathogenic *TTLL5* variants. The probands are: subject P1 [II:3, family F1; c.1782del;p.(Asp594Glufs*29)], subject P2 [II:4, family F2; c.349C > T;p.(Gln117*)], subject P3 [II:3, family F3; c.2132_2133insGATA;p.(Met712IleAspfs*15)], subject P4 [II:4, family F4; c.1627G > A;p.(Glu543Lys)], subject P5 [II:4, family F5; c.2266A > T;p.(Ile756Phe)], and subject P6 [IV:14, family F6; c.1627G > A;p.(Glu543Lys)].

based Next-Generation Sequencing screening [the IROme (12)], we performed whole-genome sequencing (WGS) of the patient's DNA. This latter procedure resulted in more than 4 million DNA variants with respect to the human reference genome (Build hg19). These were evaluated by the use of an internal *in-silico* pipeline assessing their frequency in the general population, quality, etc. (Supplementary Material, Table S1), as well as their presence within autozygous regions (Supplementary Material, Fig. S1). At the end of this process, we were left with 19 variants (7 in autozygous regions), including c.1782delT in *TTLL5* (Fig. 3), a gene known to be involved in microtubule posttranslational modifications and associated with ciliary microtubule stabilization (13). The variant was in exon 20 and consisted of a 1-bp deletion causing a frameshift starting from codon 594 and terminating with the creation of a premature stop triplet 29 codons downstream [p.(Asp594Glufs*29)]. It was also not detected in the genome of 400 healthy controls from the same geographic region of Switzerland [data from the CoLaus study (14)], and from publicly available databases [ExAC (15), dbSNP (16)]. Importantly, this DNA change localized to a region of chromosome 14 (75,986,579-80,875,911, Build hg19) showing clear autozygosity (Supplementary Material, Fig. S1) in P1's genome.

Because of the possible involvement of TTLL5 in extraocular ciliary functions, the patient underwent more detailed clinical examinations. To assess the presence of additional subtle abnormalities in organs known to be affected by ciliopathies, he was evaluated for both renal and otorhinolaryngological functions. He did not display the classical clinical features of renal ciliopathy (no polyuria/polydipsia), but chronic renal insufficiency without proteinuria (stage G3aA1) (17) was identified, associated with low-grade chronic anemia. By ultrasound, the size of the kidneys appeared to be preserved, but a small asymmetry was noted (9.6 cm on the left vs. 10.7 cm on the right side), without significant renal artery stenosis. No cysts were visible and no biopsy was performed. Altogether, the renal features were consistent with age-related decreased renal function, but low-grade and late appearance nephronophtisis cannot be fully excluded. The observed minor sensorineural hearing loss, and loss of some high frequencies, was compatible with the natural course of hearing about a person of the age of the subject (Supplementary Material, Fig. S2). The clinical examination and patient's history did not reveal any upper airway pathology necessitating further investigations for impaired mucocillary function in the sinus or the bronchi. The patient reported a history of infertility due to reduced sperm motility, diagnosed when he was in his late 20's. He could not have offspring and adopted two children. Following our findings, a new semen analysis was performed at age 75, revealing azoospermia, a sign that nonetheless could simply be related to the difficulty in obtaining an ejaculate at his current age.

Based on these findings, we extended our analyses to a number of additional cohorts of 365 patients with CD and CRD from Switzerland, Sweden, Greece, The Netherlands, and Britain. In a Swedish male patient of Iraqi descent (P2), we identified the homozygous nonsense variant c.349C > T;p.(Gln117*) by targeted Sanger sequencing of *TTLL5* (Figs. 1, F2; 3). Again, this variant was absent from controls and publicly available databases. Although the patient did not report any history of consanguinity, the occurrence of this extremely rare variant in a homozygous state suggests the presence of residual consanguinity or of a geographical founder effect, which was not tested at the genome level. The patient, aged 46 years, reported no family history of similar visual impairment. Fundus examination revealed degenerative changes, especially in the posterior pole, but more normal features in the periphery. Visual field analysis by Goldmann perimetry showed residual fields in the periphery, but a large central scotoma. Full-field ERG demonstrated residual cone and rod response, consistent with a diagnosis of cone-rod degeneration. In addition to these signs and symptoms typical of CRD, the patient had high myopia (Table 1). This subject was also infertile, but had been able to have a child by *in vitro* fertilization. His semen analysis revealed a normal spermatozoa count but, similar to P1, reduced sperm motility. He also had morphologically normal spermatozoa for 5% of the count, over three independent assays.

Following autozygome-based analysis (Supplementary Material, Fig. S1), we identified homozygous mutations in three additional patients from the Netherlands (Fig. 1, F3–5). All of them were diagnosed with CD, with full-field ERGs showing reduction of cone function but preserved rod responses (Table 1). Similar to the cases described above, the female patient P3 had a *TTLL5* truncating mutation, c.2132_2133insGATA;p.(Met712IleAspfs*15), resulting in a premature termination codon. The other two patients (P4, and P5) were males and both carried homozygous missense mutations, namely c.1627G > A;p.(Glu543Lys) and c.2266A > T;p.(Ile756Phe),

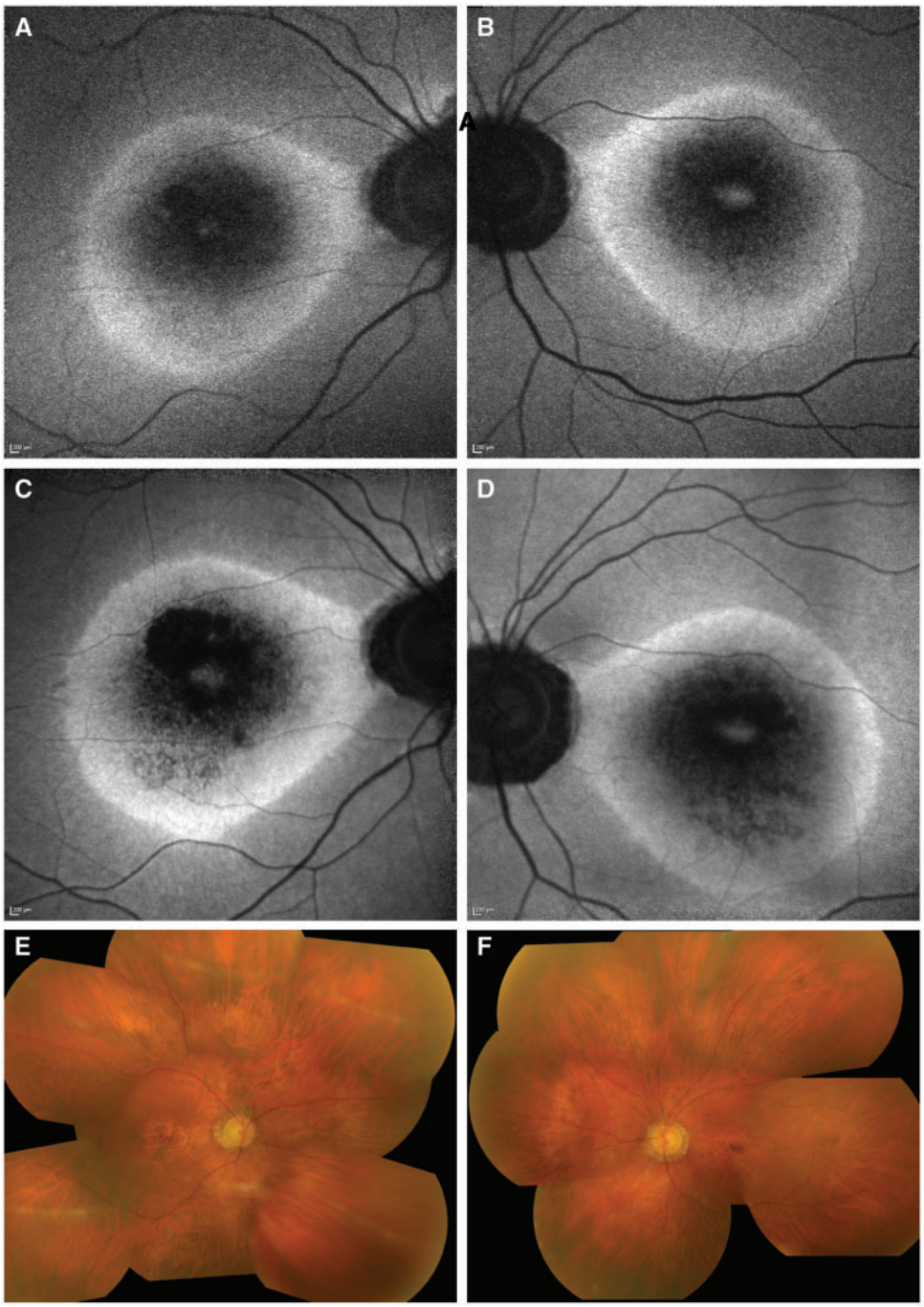

Figure 2. Fundi of index patient P1. Autofluorescence imaging of the right (**A**) and left (**B**) eye at age 66 years, showing a distinctive pattern of abnormalities, including a hyperfluorescent ring and hyperfluorescent area at the fovea surrounded by patchy hypofluorescence in both eyes. Hypofluorescence around the optic nerve was also present. The same images, obtained 6 years later (**C,D**), showed an increase of hypofluorescent areas within the ring and a mild enlargement of the hyperfluorescent ring in both eyes. Composite pictures of the fundi at age 72, showing atrophic areas around the fovea and around the optic nerve (**E,F**). Peripheral retina was within normal limits.

respectively (Fig. 3). Following colour vision testing, substantial mistakes were made in all three colour axes. All patients had a myopic refractive error, but none of them showed any additional extraocular symptoms. In particular, they did not report any fertility problems, and both male patients had offspring.

Finally, a male patient (P6) of Pakistani origin was screened by whole-exome sequencing (WES). He was a member of a consanguineous pedigree that included six additional individuals with high myopia and an acquired CD or CRD with loss of corrected visual acuity from the second decade onwards (Fig. 1, F6). In this case as well, a homozygous mutation in *TTLL5* was identified within an autozygous region in chromosome 14 (Supplementary Material, Fig. S1). It was the same missense detected above [c.1627G > A;p.(Glu543Lys), Fig. 3], which perfectly co-segregated with the disease in the three affected and two unaffected individuals for which DNA samples were available.

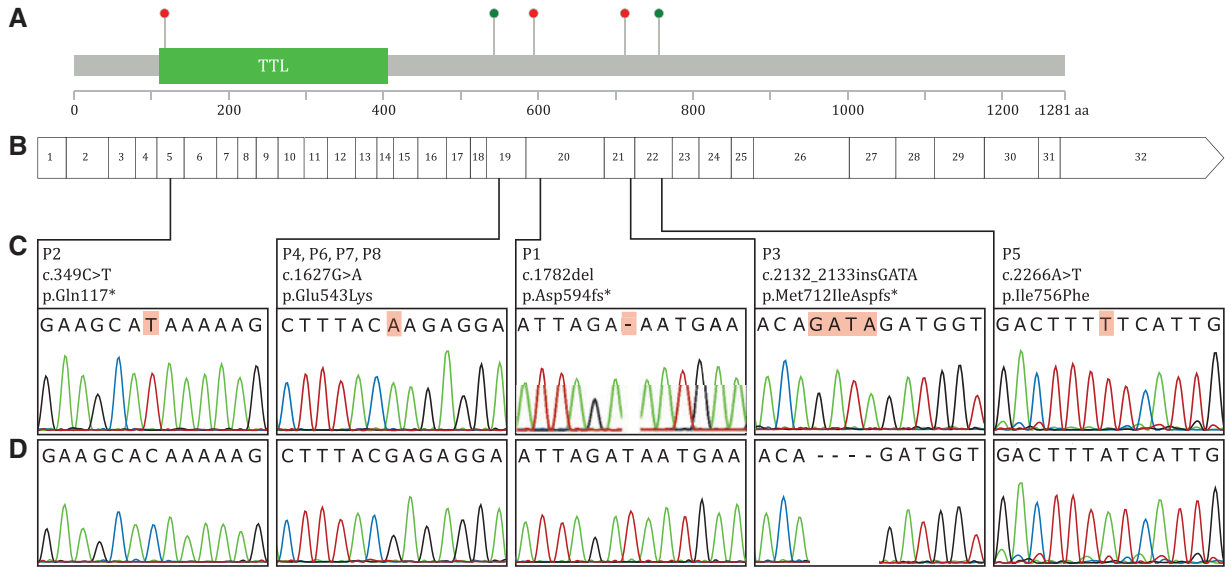

Figure 3. Mutation diagram of the TTLL5 protein (**A**), and corresponding cDNA. Red and green dots indicate truncating and missense mutations, respectively. Exons are numbered and drawn to scale (**B**) with respect to the protein sequence. The TTL domain responsible for polyglutamylation activity is indicated. Chromatograms of the mutations identified (**C**), compared to their relevant wild type sequences (**D**).

Of note, in addition to retinal dystrophy, all patients from this pedigree reported high to very-high myopia (-5 to -22 diopters) (Table 1). None of the patients reported fertility problems, and indeed patient P6 had five children.

TTLL5 RNA isoforms and expression in different tissues

According to publicly-available databases, *TTLL5* produces six protein-coding and alternatively spliced isoforms (transcripts 001, 002, 003, 016, 017, 018 of the Ensembl database GRCh37, release 84), presenting a rather widespread expression throughout different tissues and organs (UniGene). To gain insights into this topic, we investigated the composition and abundance of *TTLL5* transcripts in a panel of cadaveric organs and tissues (Fig. 4).

Our data confirmed that *TTLL5* has an extremely variable expression pattern, both in terms of isoforms and of presence in various tissues. However, qualitative and quantitative assessment of all transcripts revealed that expression of the canonical isoform 001 was overwhelmingly more abundant (more than 40-fold higher than the average of the remainder) and that expression in the retina and testis represented ∼64% of TTLL5 presence across all tissues and organs examined (31 and 33% in testis and retina, respectively; Fig. 4). Interestingly, all mutations identified in our cohort of patients affected isoform 001, and individuals with inactivating mutations showed reduced fertility (Table 1).

TTLL5 mRNA level in the index patient P1

Since mutations leading to premature termination codons trigger nonsense-mediated mRNA decay (NMD) and result in no or in short-lived transcripts (18), we analysed expression of *TTLL5* in skin fibroblasts from patient P1, displaying retinal degeneration and infertility. Quantitative real time PCR (q-PCR) resulted in a dramatically reduced detection of the transcript of interest as compared to a healthy control fibroblast mRNA (∼10%; Fig. 4).

TTLL5 protein in ciliated fibroblasts, retina, and spermatozoa

To better understand the role of TTLL5 with respect to the cellular cilium, we analysed control fibroblasts following serum starvation, a procedure that induces ciliogenesis. Immunofluorescence analysis revealed the clear localization of TTLL5 at both centrioles (Fig. 5, panels A–D).

Subsequently, we performed immunofluorescence analyses in the retina and sperm cells from rat and human, respectively (Fig. 5, panels E-G). In agreement with previous results in mouse and human (5), the anti-TTLL5 antibody decorated the inner segment of photoreceptors in proximity of the basal body and the connecting cilium, suggesting that TTLL5 may in fact play its functions at the base of the photoreceptor primary cilium.

Staining of mature human spermatozoa also indicated for the first time a clear centrosomal localization of TTLL5, with no overlap with the polyglutamylated α- and β-tubulin of the flagellum.

Discussion

Both primary (or immotile) and motile cilia play crucial roles in the normal function of most tissues of the human body. These tiny hair-like organelles participate in a wide range of cellular functions during development, tissue morphogenesis and homeostasis. It is therefore not surprising that mutations in ciliary genes are often associated with a broad range of conditions, classified as ciliopathies, either involving single organs or causing syndromic phenotypes (8). Some examples of diseases affecting primary cilia are polycystic kidney disease, Usher syndrome, retinitis pigmentosa, Bardet-Biedl and Joubert syndromes (19–22). On the other hand, motile cilia defects have been shown to be causative for Kartagener syndrome and allied diseases, collectively grouped under the disease spectrum of primary ciliary dyskinesias.

Cilia and flagella, highly conserved in their core structure, are ancestral organelles composed of more than 650 proteins (10,23). The building units of both ciliary and flagellar

Table 1. Patients with TTLL5 mutations and clinical features

Family	Patient	TTLL5 protein change	Zygosity	Sex	Age at last examination	Visual acuity	Correction	Full field ERG at last examination		Macula	Periphery	Other features
								cone response	rod response			
F1	P1	c.1782del; p.Asp594Glufs*29	hom	M	75	0.05	−3.6	absent	reduced	atrophy	normal	azoospermia
F2	P2	c.349C>T; p.Gln117*	hom	M	46	0.05	−10.00	residual	residual	atrophy	minor changes	reduced motility of sperm; normal anterior eye segment
F3	P3	c.2132_2133insGATA; p.Met712IleAspfs*15	hom	F	58	0.16	−3	reduced	normal		normal	
F4	P4	c.1627G>A; p.Glu543Lys	hom	M	61	0.03	−5	absent	normal	atrophy	normal	
F5	P5	c.2266A>T; p.Ile756Phe	hom	M	38	0.33	−8	absent	normal	pigmentary changes	normal	
F6	P6	c.1627G>A; p.Glu543Lys	hom	M	53	NA	−8.00	NA	NA	atrophy	pigmentary changes	phthisical right eye
	P7	c.1627G>A; p.Glu543Lys	hom	M	38	NA	−5.00	NA	NA	NA	NA	posterior subcapsular cataract
	P8	c.1627G>A; p.Glu543Lys	hom	M	18	NA	−22.00	NA	NA	NA	NA	fairly normal retina

microtubules, α- and β-tubulin, are subject to post-translational modifications, accomplished by enzymes catalyzing different reactions such as the generation of Δ2-tubulin, acetylation (24), tyrosination (25), polyglutamylation (26) and polyglycilation (27,28). Among members of the TTLL superfamily there are glutamylases and glycilases (29–31). TTLL5 initiates the formation of side chains within the C-terminal tail of α- and β-tubulin, with a preference for α-tubulin (32), and current models indicate that the role of polyglutamylation is to provide the necessary conditions for proper MT-MAPs (microtubule and microtubule-associated proteins) interactions. Studies have shown that polyglutamylation exerts differential regulation by selectively recruiting different MAPs: MAP1B, MAP2, tau, and neuronal kinesins have higher affinity for tubulins with 1-3 glutamyl units, whereas MAP1A has higher affinity for longer side chains (25,26,28). Moreover, it has been shown that masking polyglutamylated sites with a specific anti-polyglutamylated tubulin antibody (GT335) affects the amplitude of flagellar beating in sea urchin sperm axonemes, suggesting a key role of polyglutamylated sites for interaction with ciliary dyneins (33). Centriole stability was also shown to be influenced by the degree of polyglutamylation, and GT335 antibody-loaded HeLa cells showed a complete transient disappearance of the centriole pair (13). Finally, members of the TTLL family, Ttll3 and Ttll6, play a role in cilia structure and motility in zebrafish (34). All TTLL proteins have a preference for either α- or β-tubulin and participate to either initiation or elongation of the polyglutamyl side chain. TTLL5, together with TTLL4 and TTLL7, initiates polyglutamylation, while other members function in the elongation of the polyglutamyl side chain or in the initiation or the elongation of polyglycylation.

Specific patterns of modifications on microtubules might be responsible for various functions. In the case of polyglutamylation, the side chains are built within the carboxy-terminal tail of tubulin, where the binding sites of motor and MT-associated proteins (MAPs) are also found. Thus, it is plausible that the interaction of MTs with such proteins might depend on specific patterns of modifications (35). Additional studies highlighted the importance of polyglutamylation for the proper beating of airway cilia (36), as well as for providing a molecular traffic sign required by motor proteins in order to maintain continuous synaptic transmission (37). Major evidence of the implication of polyglutamylation in photoreceptor ciliary function was recently reported (7), showing that *Ttll5*$^{-/-}$ mice developed a similar retinal phenotype to *Rpgr*$^{-/-}$ mice, a known mouse model for retinitis pigmentosa. In addition, *Ttll5*$^{-/-}$ mice display strongly reduced glutamylation of RPGR^{ORF15}, a retina-specific variant of RPGR (38). Altogether, current evidence strongly supports the notion that the presence and length of polyglutamyl side chains, not only on tubulin but also on other substrates, is crucial for proper functioning of both motile and immotile cilia.

In our work we show that mutations in a gene involved in the polyglutamylation of α-tubulin is associated with defects in the retina and spermatozoa. Clinically, these molecular phenotypes translate into cone-first CRD and reduced sperm motility, likely due to the functional impairment of the primary cilium and the flagellum, respectively. Our assumption is supported by immunofluorescence data, demonstrating that TTLL5 localizes at the basal body of the cilia in photoreceptors, as well as at the base of the spermatozoal axoneme and in ciliated skin fibroblasts. Moreover, we reveal that the highest levels of expression of the major *TTLL5* protein-coding isoform is in the retina and testis. It is also very interesting to note that, in terms of fertility and *TTLL5* pathogenic variants, there is an apparent

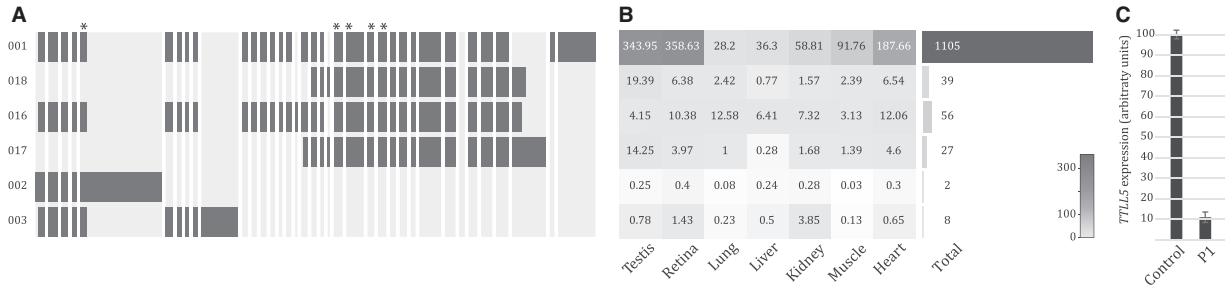

Figure 4. Relative expression of *TTLL5* isoforms and their expression. *TTLL5* has six known alternative transcripts (001, 002, 003, 016, 017, and 018), resulting from the splicing of the exons indicated here in dark grey (**A**). Their expression within seven different human tissues, measured by quantitative real time PCR, is indicated by both numerical values and shades of grey (**B**). Although all isoforms seem to be widely expressed, isoform 001 is the most prominent one, among all tissues considered ('Total' column). Asterisks show the position of the mutations identified in this work. *TTLL5* isoform 001 expression in fibroblasts of the index patient P1 vs. a control, by quantitative PCR (**C**). *TTLL5* mRNA amounts were normalized with respect to the housekeeping gene *HPRT1*.

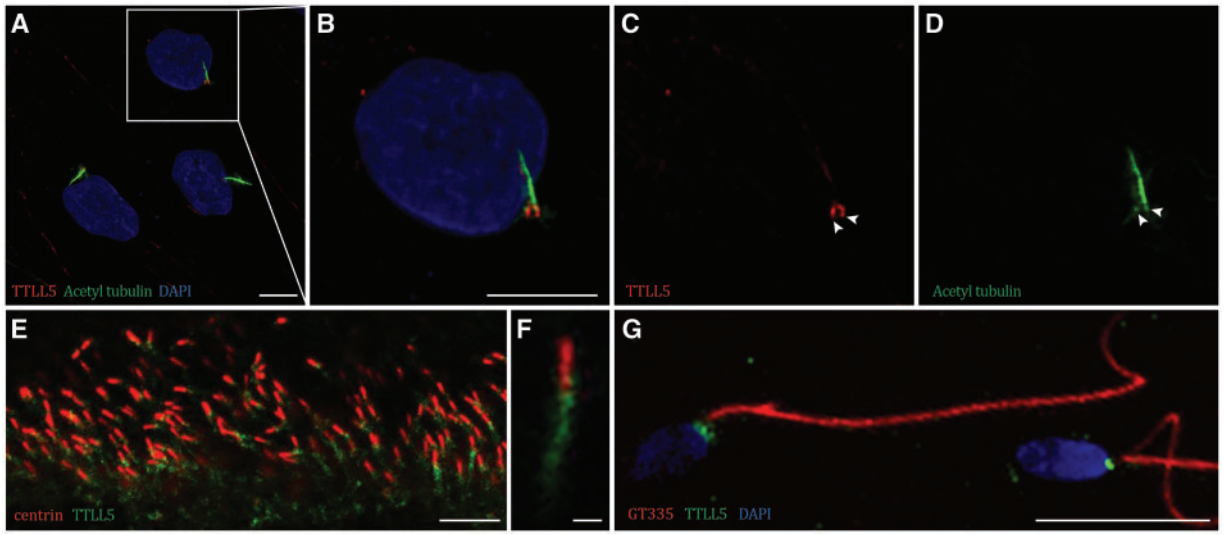

Figure 5. Immunofluorescence staining of ciliated control human skin fibroblasts (**A-D**). TTLL5 co-localizes with acetylated tubulin at the centrioles, as indicated by arrowheads (C,D). Immunofluorescence in rat retina sections (**E**, and magnified cilium in **F**) and in control human spermatozoon (**G**). TTLL5 decorates the basal body in photoreceptors and the centrioles in spermatozoa. Scale bars: A-E, 5 μm; F, 1 μm; G, 20 μm.

genotype/phenotype correlation, which seems to be irrelevant for retinal degeneration. In other words, the phenotype elicited by *TTLL5* pathogenic changes appears to depend on mutation classes. Missense variants are seemingly associated with a non-syndromic phenotype that is limited to the retina, whereas inactivating mutations appear to disrupt the functions of both photoreceptors and spermatozoa, thus defining a novel allele-specific syndrome. Yet, three male patients with truncating *TTLL5* mutations were previously reported having offspring (5), raising the possibility of variable expressivity or reduced penetrance of this class of mutations. In support of the latter hypothesis, *Ttll5* knockout mice display extremely reduced but not completely abolished fertility (6). Alternatively, this genotype/phenotype correlation in our cohort could also be coincidental. The association of *TTLL5* mutations with severe myopia is another intriguing hypothesis that warrants additional investigation in a larger cohort of patients, especially given the complex pattern of inheritance of nearsightedness in humans.

In conclusion, we show that mutations in *TTLL5* are associated with a newly-defined syndrome affecting vision and the male reproductive system. Despite the fact that cilia and flagella have different morphologies and functions, they may share similar physiological mechanisms, and the enzymatic reaction of polyglutamylation performed by TTLL5 may be one of these common elements.

Materials and Methods

Patients and controls

Patient P1 was recruited from the Jules Gonin Ophthalmic Hospital (Lausanne, Switzerland); and patient P2 from the Department of Ophthalmology of Lund University Hospital (Lund, Sweden). Patients P3, P4 and P5 were recruited from the Radboud University Medical Center (Nijmegen, The Netherlands) and the Erasmus University Medical Center (Rotterdam, The Netherlands). Patients P6-8 were sampled by author MMK, an ophthalmologist based at St James's University Hospital (Leeds, England), while on a field trip to Pakistan. DNA of all subjects was extracted from peripheral blood leukocytes. A control sperm sample was provided by a healthy donor. Our research has been conducted in accordance with the tenets of the Declaration of Helsinki and was approved by the Institutional Review Boards of our respective Organizations.

Clinical evaluation

For patients P1-5, ophthalmologic examination included assessment of BCVA, slit-lamp examination, funduscopy, fundus photography, and optical coherence tomography. Full-field ERGs were also recorded, as prescribed by the International Society for Clinical Electrophysiology of Vision (ISCEV).

For patients P6-8, ophthalmologic assessment was limited to slit-lamp examination and fundus inspection using direct and indirect ophthalmoscopy through dilated pupils. Owing to the non-hospital setting, electrodiagnostic and other testing was not available. Visual acuity was recorded together with a history of nyctalopia or photoaversion.

Semen analysis was carried out for patients P1 and P2 by standard procedures of andrology laboratories, and according to WHO guidelines (39). For P1 patient, two Leja chambers (Leja) filled with 6 μl of semen were entirely scanned under phase contrast microscopy to confirm the absence of spermatozoa. Additional clinical features were assessed only for patient P1, due to substantial problems in getting back to the other probands. These tests included a thorough otorhinolaryngologic examination assessing structure and function of the nasopharyngeal mucosa, the ear canal and the hearing (by pure-tone audiometry), as well as a full renal examination, including a complete checkup of renal function, urine and blood analysis, assessment of blood pressure, and ultrasonography. Analyses involving other tissues and organs known to be involved in other ciliopathies were not performed due to a negative clinical history: normal body mass index, no respiratory complains, no metabolic disturbance and no skeletal abnormalities.

Whole-genome and whole-exome sequencing

WGS in the Swiss index patient P1 was performed using 4 μg of DNA. Sequencing was performed by Complete Genomics Inc. (Mountain View, CA, USA), as described previously (40). Genetic variants were identified using v2.0 of the Complete Genomics pipeline (41). WES was performed for proband P6 using 3 μg of DNA. Protein-coding regions were captured using the SureSelect All Exon v4 kit (Agilent) and paired-end sequencing was performed using the Illumina HiSeq 2500 platform. Single nucleotide variants and small insertions or deletions were detected using the Genome Analysis Tool Kit (GATK v2.4.7) software package, using the Best Practice Guidelines identified by the developers (42). The pathogenicity of genetic variants detected through WGS and WES were assessed after functional annotation through ANNOVAR (43).

Homozygosity mapping

Genomic regions with high homozygosity were determined using the free web-based tool HomozygosityMapper (44).

Mutation screening

Primer pairs for *TTLL5* exons and flanking intron boundaries were designed using the CLCbio Genomics Workbench (Qiagen, Supplementary Material, Table S2). PCR amplification was performed in a 20 μl total volume containing 10 ng genomic DNA, 1x GoTaq buffer, 0.1 mM dNTPs, 10 μM of each primer, and 5 U/μl of GoTag polymerase (Promega). PCR products were purified (ExoSAP-IT, USB) and a sequencing reaction was performed in a total volume of 5 μl using 1 μl primer 3.3 μM, 0.5 μl BigDye Terminator v1.1, and 1 μl of the provided Buffer (Applied Biosystems).

Antibodies

Commercial goat polyclonal anti-TTLL5 antibody (Santa Cruz Biotechnology Inc), raised against a peptide mapping near the C-terminus of TTLL5 human origin, was used at a 1:100 dilution. Mouse monoclonal anti-centrin clone 20H5 antibody was purchased from Millipore and used at a dilution of 1:1000. Anti-polyglutamylated tubulin GT335 and monoclonal anti-acetylated tubulin antibodies were provided by Dr C. Janke (Institut Curie, Orsay, France) and purchased from Sigma-Aldrich, respectively. Secondary donkey anti-goat antibodies conjugated with Alexa Fluor 488 were purchased from Invitrogen and secondary goat anti-mouse antibodies (Life Technologies) were conjugated with Alexa Fluor 594 (1:1000).

Fibroblast immortalization and culture

Primary skin fibroblasts were immortalized with exogenous hTERT by the use of pLOX-TERT-iresTK (45) and grown in DMEM(1x) + 1g/L D-glucose L-Glutamine Pyruvate (Gibco), supplemented with 10% FBS, 1% penicillin-streptomycin, and 1% fungizone, adapted from previously published protocols (46).

Immunofluorescence

Immunofluorescence was performed for TTLL5 localization in human control spermatozoa and rat retinal sections. The sperm staining procedure used was adapted from a previously published protocol (47). After washing five times with PBS 1X in a 15 ml Falcon tube and centrifugation steps of 5' at 800g, all at room temperature (RT), the semen pellet was resuspended and fixed with 4% (v/w) PFA in PBS, and incubated for 30 min on ice. The sample was then washed three times with PBS and stored at 4 °C for future use. The immunostaining procedure used 20 μl aliquots of fixed sperm cells, transferred to a 1.5 μl Eppendorf tube. Blocking was done for 30 min at RT in 100 μl PBS containing 3% (w/v) BSA (PBSA). Primary antibody incubation was performed with specified dilutions in 100 μl PBSA, overnight at 4 °C. Samples were washed three times with PBS containing 0.1% (v/v) TX100 (PBST). Secondary antibody incubation for 30 min was carried out at RT in 100 μl PBSAT [PBST containing 3% (w/v) BSA and 0.1% (v/v) TX100]. After three washes with PBST and two washes with PBS the final pellet was resuspended in PBS and 5 μl were placed on a slide. 5 μl DAPI vectashield were added to the sample, which was then coverslipped and fixed with nail polish.

Unfixed Sprague-Dawley rat eyes and C57BL/6J mouse eyes were isolated and soaked for 3 h in PBS containing 30% sucrose. Eyes were embedded in Yazulla medium (30% egg albumen and 3% gelatin in water) and cryosectioned (12 μm) onto Superfrost Plus slides (Thermo Scientific). Sections were washed three times with PBS and a stepwise procedure was followed similar to that described for sperm immunostaining, the only difference being that this was carried out on the slide and with lower volumes.

Quantitative real time PCR

Primer pairs used for q-PCR are listed in Supplementary Material, Table S3. The q-PCR product was visualized on 1%

agarose gel to verify the primer's specificity. A standard curve using a control cDNA template prepared from human normal tissues total RNA (BioChain) was used to test the efficiency of each primer pair. *HPRT1* was used as a normalization control, as described (48). Amplification was performed using the SYBR Green PCR Master Mix (Applied Biosystems).

Supplementary Material

Supplementary Material is available at *HMG* online.

Acknowledgements

We would like to thank the patients and their families who participated in this study.

Conflict of Interest statement. None declared.

Funding

This work was supported by grants from the Swiss National Science Foundation to CR [grant numbers 138346, 156260], the Foundation Fighting Blindness USA to FPMC [grant number C-GE-0811-0545-RAD01], and RP Fighting Blindness and Fight For Sight [RP Genome Project GR586]. MEE was funded by an Egyptian Government Scholarship. Family F6 was analysed by the UK Inherited Retinal Disease Consortium.

References

1. Hamel, C.P. (2007) Cone rod dystrophies. *Orphanet J. Rare Dis.*, **2**, 7.
2. Berson, E.L., Gouras, P. and Gunkel, R.D. (1968) Progressive cone-rod degeneration. *Arch. Ophthalmol.*, **80**, 68–76.
3. Berson, E.L., Gouras, P. and Gunkel, R.D. (1968) Progressive cone degeneration, dominantly inherited. *Arch. Ophthalmol.*, **80**, 77–83.
4. Roosing, S., Thiadens, A.A., Hoyng, C.B., Klaver, C.C., den Hollander, A.I. and Cremers, F.P. (2014) Causes and consequences of inherited cone disorders. *Prog. Retin. Eye Res.*, **42**, 1–26.
5. Sergouniotis, P.I., Chakarova, C., Murphy, C., Becker, M., Lenassi, E., Arno, G., Lek, M., MacArthur, D.G., Consortium, U.C.E., Bhattacharya, S.S., *et al.* (2014) Biallelic variants in TTLL5, encoding a tubulin glutamylase, cause retinal dystrophy. *Am. J. Hum. Genet.*, **94**, 760–769.
6. Lee, G.S., He, Y., Dougherty, E.J., Jimenez-Movilla, M., Avella, M., Grullon, S., Sharlin, D.S., Guo, C., Blackford, J.A., Jr., Awasthi, S., *et al.* (2013) Disruption of Ttll5/stamp gene (tubulin tyrosine ligase-like protein 5/SRC-1 and TIF2-associated modulatory protein gene) in male mice causes sperm malformation and infertility. *J. Biol. Chem.*, **288**, 15167–15180.
7. Sun, X., Park, J.H., Gumerson, J., Wu, Z., Swaroop, A., Qian, H., Roll-Mecak, A. and Li, T. (2016) Loss of RPGR glutamylation underlies the pathogenic mechanism of retinal dystrophy caused by TTLL5 mutations. *Proc. Natl Acad. Sci. U. S. A*, **113**, E2925–E2934.
8. Hildebrandt, F., Benzing, T. and Katsanis, N. (2011) Ciliopathies. *N. Engl. J. Med.*, **364**, 1533–1543.
9. Waters, A.M. and Beales, P.L. (2011) Ciliopathies: an expanding disease spectrum. *Pediatr. Nephrol.*, **26**, 1039–1056.
10. Fliegauf, M., Benzing, T. and Omran, H. (2007) When cilia go bad: cilia defects and ciliopathies. *Nat. Rev. Mol. Cell Biol.*, **8**, 880–893.
11. Hildebrandt, F., Attanasio, M. and Otto, E. (2009) Nephronophthisis: disease mechanisms of a ciliopathy. *J. Am. Soc. Nephrol.*, **20**, 23–35.
12. Schorderet, D.F., Bernasconi, M., Tiab, L., Favez, T. and Escher, P. (2014) IROme, a new high-throughput molecular tool for the diagnosis of inherited retinal dystrophies-a price comparison with Sanger sequencing. *Adv. Exp. Med. Biol.*, **801**, 171–176.
13. Bobinnec, Y., Khodjakov, A., Mir, L.M., Rieder, C.L., Edde, B. and Bornens, M. (1998) Centriole disassembly in vivo and its effect on centrosome structure and function in vertebrate cells. *J. Cell Biol.*, **143**, 1575–1589.
14. Firmann, M., Mayor, V., Vidal, P.M., Bochud, M., Pecoud, A., Hayoz, D., Paccaud, F., Preisig, M., Song, K.S., Yuan, X., *et al.* (2008) The CoLaus study: a population-based study to investigate the epidemiology and genetic determinants of cardiovascular risk factors and metabolic syndrome. *BMC Cardiovasc. Disord.*, **8**, 6.
15. Lek, M., Karczewski, K., Minikel, E., Samocha, K., Banks, E., Fennell, T., O'Donnell-Luria, A., Ware, J., Hill, A., Cummings, B., *et al.* (2015) Analysis of protein-coding genetic variation in 60,706 humans. *Nature.*, **536**, 285–291.
16. Sherry, S.T., Ward, M.H., Kholodov, M., Baker, J., Phan, L., Smigielski, E.M. and Sirotkin, K. (2001) dbSNP: the NCBI database of genetic variation. *Nucleic Acids Res.*, **29**, 308–311.
17. KDIGO. (2013) Clinical practice guideline for the evaluation and management of chronic kidney disease. *Kidney Int Suppl.*, **3**, 150.
18. Hentze, M.W. and Kulozik, A.E. (1999) A perfect message: RNA surveillance and nonsense-mediated decay. *Cell*, **96**, 307–310.
19. Badano, J.L., Mitsuma, N., Beales, P.L. and Katsanis, N. (2006) The ciliopathies: an emerging class of human genetic disorders. *Annu. Rev. Genomics Hum. Genet.*, **7**, 125–148.
20. Zaghloul, N.A. and Katsanis, N. (2009) Mechanistic insights into Bardet-Biedl syndrome, a model ciliopathy. *J. Clin. Invest.*, **119**, 428–437.
21. Forsythe, E. and Beales, P.L. (2013) Bardet-Biedl syndrome. *Eur. J. Hum. Genet.*, **21**, 8–13.
22. Falk, N., Losl, M., Schroder, N. and Giessl, A. (2015) Specialized Cilia in Mammalian Sensory Systems. *Cells*, **4**, 500–519.
23. Carvalho-Santos, Z., Azimzadeh, J., Pereira-Leal, J.B. and Bettencourt-Dias, M. (2011) Evolution: Tracing the origins of centrioles, cilia, and flagella. *J. Cell Biol.*, **194**, 165–175.
24. Piperno, G. and Fuller, M.T. (1985) Monoclonal antibodies specific for an acetylated form of alpha-tubulin recognize the antigen in cilia and flagella from a variety of organisms. *J. Cell Biol.*, **101**, 2085–2094.
25. Gundersen, G.G. and Bulinski, J.C. (1986) Distribution of tyrosinated and nontyrosinated alpha-tubulin during mitosis. *J. Cell Biol.*, **102**, 1118–1126.
26. Edde, B., Rossier, J., Le Caer, J.P., Desbruyeres, E., Gros, F. and Denoulet, P. (1990) Posttranslational glutamylation of alpha-tubulin. *Science*, **247**, 83–85.
27. Westermann, S. and Weber, K. (2003) Post-translational modifications regulate microtubule function. *Nat. Rev. Mol. Cell Biol.*, **4**, 938–947.
28. Janke, C. and Kneussel, M. (2010) Tubulin post-translational modifications: encoding functions on the neuronal microtubule cytoskeleton. *Trends Neurosci.*, **33**, 362–372.

29. Boucher, D., Larcher, J.C., Gros, F. and Denoulet, P. (1994) Polyglutamylation of tubulin as a progressive regulator of in vitro interactions between the microtubule-associated protein Tau and tubulin. *Biochemistry*, **33**, 12471–12477.
30. Larcher, J.C., Boucher, D., Lazereg, S., Gros, F. and Denoulet, P. (1996) Interaction of kinesin motor domains with alpha- and beta-tubulin subunits at a tau-independent binding site. Regulation by polyglutamylation. *J. Biol. Chem.*, **271**, 22117–22124.
31. Bonnet, C., Boucher, D., Lazereg, S., Pedrotti, B., Islam, K., Denoulet, P. and Larcher, J.C. (2001) Differential binding regulation of microtubule-associated proteins MAP1A, MAP1B, and MAP2 by tubulin polyglutamylation. *J. Biol. Chem.*, **276**, 12839–12848.
32. Janke, C., Rogowski, K., Wloga, D., Regnard, C., Kajava, A.V., Strub, J.M., Temurak, N., van Dijk, J., Boucher, D., van Dorsselaer, A., *et al.* (2005) Tubulin polyglutamylase enzymes are members of the TTL domain protein family. *Science*, **308**, 1758–1762.
33. Gagnon, C., White, D., Cosson, J., Huitorel, P., Edde, B., Desbruyeres, E., Paturle-Lafanechere, L., Multigner, L., Job, D. and Cibert, C. (1996) The polyglutamylated lateral chain of alpha-tubulin plays a key role in flagellar motility. *J. Cell Sci.*, **109**, 1545–1553.,
34. Pathak, N., Austin, C.A. and Drummond, I.A. (2011) Tubulin tyrosine ligase-like genes ttll3 and ttll6 maintain zebrafish cilia structure and motility. *J. Biol. Chem.*, **286**, 11685–11695.
35. Janke, C., Rogowski, K. and van Dijk, J. (2008) Polyglutamylation: a fine-regulator of protein function? 'Protein Modifications: beyond the usual suspects' review series. *EMBO Rep.*, **9**, 636–641.
36. Ikegami, K., Sato, S., Nakamura, K., Ostrowski, L.E. and Setou, M. (2010) Tubulin polyglutamylation is essential for airway ciliary function through the regulation of beating asymmetry. *Proc. Natl Acad. Sci. U. S. A*, **107**, 10490–10495.
37. Ikegami, K., Heier, R.L., Taruishi, M., Takagi, H., Mukai, M., Shimma, S., Taira, S., Hatanaka, K., Morone, N., Yao, I., *et al.* (2007) Loss of alpha-tubulin polyglutamylation in ROSA22 mice is associated with abnormal targeting of KIF1A and modulated synaptic function. *Proc. Natl Acad. Sci. U. S. A*, **104**, 3213–3218.
38. Vervoort, R., Lennon, A., Bird, A.C., Tulloch, B., Axton, R., Miano, M.G., Meindl, A., Meitinger, T., Ciccodicola, A. and Wright, A.F. (2000) Mutational hot spot within a new RPGR exon in X-linked retinitis pigmentosa. *Nat. Genet.*, **25**, 462–466.
39. WHO. (2010) WHO laboratory manual for the examination and processing of human semen.
40. Drmanac, R., Sparks, A.B., Callow, M.J., Halpern, A.L., Burns, N.L., Kermani, B.G., Carnevali, P., Nazarenko, I., Nilsen, G.B., Yeung, G., *et al.* (2010) Human genome sequencing using unchained base reads on self-assembling DNA nanoarrays. *Science*, **327**, 78–81.
41. Carnevali, P., Baccash, J., Halpern, A.L., Nazarenko, I., Nilsen, G.B., Pant, K.P., Ebert, J.C., Brownley, A., Morenzoni, M., Karpinchyk, V., *et al.* (2012) Computational techniques for human genome resequencing using mated gapped reads. *J. Comput. Biol.*, **19**, 279–292.
42. DePristo, M.A., Banks, E., Poplin, R., Garimella, K.V., Maguire, J.R., Hartl, C., Philippakis, A.A., del Angel, G., Rivas, M.A., Hanna, M., *et al.* (2011) A framework for variation discovery and genotyping using next-generation DNA sequencing data. *Nat. Genet.*, **43**, 491–498.
43. Wang, K., Li, M. and Hakonarson, H. (2010) ANNOVAR: functional annotation of genetic variants from high-throughput sequencing data. *Nucleic Acids Res.*, **38**, e164.
44. Seelow, D., Schuelke, M., Hildebrandt, F. and Nurnberg, P. (2009) HomozygosityMapper–an interactive approach to homozygosity mapping. *Nucleic Acids Res.*, **37**, W593–W599.
45. Salmon, P., Oberholzer, J., Occhiodoro, T., Morel, P., Lou, J. and Trono, D. (2000) Reversible immortalization of human primary cells by lentivector-mediated transfer of specific genes. *Mol. Ther.*, **2**, 404–414.
46. van Karnebeek, C.D., Bonafe, L., Wen, X.Y., Tarailo-Graovac, M., Balzano, S., Royer-Bertrand, B., Ashikov, A., Garavelli, L., Mammi, I., Turolla, L., *et al.* (2016) NANS-mediated synthesis of sialic acid is required for brain and skeletal development. *Nat. Genet.*, **48**, 777–784.
47. Nishimura, H., Gupta, S., Myles, D.G. and Primakoff, P. (2011) Characterization of mouse sperm TMEM190, a small transmembrane protein with the trefoil domain: evidence for colocalization with IZUMO1 and complex formation with other sperm proteins. *Reproduction*, **141**, 437–451.
48. Hoggart, C.J., Venturini, G., Mangino, M., Gomez, F., Ascari, G., Zhao, J.H., Teumer, A., Winkler, T.W., Tsernikova, N., Luan, J., *et al.* (2014) Novel approach identifies SNPs in SLC2A10 and KCNK9 with evidence for parent-of-origin effect on body mass index. *PLoS Genet.*, **10**, e1004508.